

Electrophoresis in Polymer Solutions: Mechanisms of Molecular Sieving

Sergey P. Radko and Andreas Chrambach*

Section on Macromolecular Analysis, Laboratory of Theoretical and Physical Biology, National Institute of Child Health and Human Development, National Institutes of Health, Bethesda, Maryland 20892

Received: April 30, 1996; In Final Form: August 18, 1996[⊗]

Passage of rigid, “spherical” proteins in the range of 2–5 nm radius, R (40–500 kDa molecular weight), through semidilute solutions of a representative polymer, polyethylene glycol in the molecular weight range of $(0.6–8) \times 10^6$, gives rise to a size dependent retardation (“molecular sieving”) analogous to that in a porous network composed of random planes. The average distance between those planes being equal to the screening length, ξ , the retardation can be described by $\log(\mu/\mu_0) = -(ARc^{0.75})$ where A is a constant dependent on solvent and type of monomer and c is the polymer concentration.

1. Introduction

Solutions of entangled polymers (or semidilute solutions) constitute a continuous spatial network due to steric interactions between the polymer chains (“entanglements”) and can be applied as a matrix for electrophoretic separation of particles differing in size and shape (“molecular sieving”) in analogy to gels.¹ Recently they have gained practical importance in view of the widespread acceptance of capillary electrophoresis permitting separation with an acceptable level of peak dispersion and correspondingly good resolution² which is due to particular anticonvective and heat dissipation properties of thin capillaries. In spite of that importance, the mechanisms of molecular sieving in semidilute solutions are not fully understood.

For gel electrophoresis, different sieving mechanisms have been proposed depending on the properties of the particles undergoing electrophoretic migration. The sieving of linearly elongated, entangled macromolecules (e.g. DNA) is described in terms of the reptation model (e.g., ref 3 and references therein). The model developed by Arvanitidou et al. for a dilute gel⁴ may be the most suitable to describe the sieving mechanism for stiff rodlike macromolecules and flexible chains. For rigid spherical macromolecules, the Ogston model^{5–7} has been applied to describe the mechanism governing molecular sieving. In addition to these analytical models of gel permeation, it has also been the subject of computer simulations (e.g. refs 8 and 9). All models and simulations consider a gel as an array of geometrically idealized obstacles, in other words, a porous medium with pores equal to the spacing between obstacles.

Theoretical approaches to the sieving mechanisms in semidilute solutions were pioneered by Grossmann and Soane.¹⁰ They considered the solutions as a porous medium with an average pore size equal to the “mesh” size of a polymer network, defined as the screening length, ξ , an essential parameter underlying the theory of semidilute solutions and conceived as the average distance between entanglement points.¹¹ Thus theories of molecular sieving by electrophoretic methods have been directly transposed from gels to polymer solutions.^{2,12,10,13}

The present study focuses on the simplest case of the electrophoretic migration of rigid particles of approximately spherical shape (native proteins) through semidilute polymer solutions. Using the analogy between gels and the semidilute

solutions,¹⁰ application of the Ogston model in that case appeared justified. The model views the gel as a random array of inert, geometrically idealized obstacles (random planes, fibers, or “points”) and considers the occupation of the fractional available space in the network by particles modeled as spheres of radius R .⁶ The model rests on the assumption of Morris¹⁴ that the ratio of restricted mobility, μ , to free mobility, μ_0 , is equal to the fractional volume available to a spherical particle in the random array of obstacles. The expression for the ratio μ/μ_0 may be written in a general form

$$\mu/\mu_0 = \exp[-(kR/d)^m] \quad (1)$$

where the exponent m is equal to 1, 2, and 3 for the plane, fiber, and point shaped obstacles, respectively, d is the mean distance within the spaces formed by the array, and k is a numerical coefficient dependent on the obstacle geometry.

For gel electrophoresis, the model of a random fiber network appears to be the most physically realistic. For such a network the Ogston model yields⁶

$$\mu/\mu_0 = \exp[-(\pi Ln)R^2] \quad (2)$$

where L is the uniform fiber length and n is the average number of those lengths per unit volume. Equation 2 can be rewritten in terms of the retardation coefficient, K_R , and gel concentration, T (%), as

$$\log(\mu/\mu_0) = -K_R T \quad (3)$$

The model has gained indirect support from the experimental evidence for linear “Ferguson plots” ($\log(\mu/\mu_0)$ vs T) and the square root dependence of K_R on R in the polyacrylamide gel electrophoresis of proteins.^{6,7}

The present work aims at answering the questions of (i) how the concept of a mesh size of a polymer network in solution can be fitted into the Ogston model and (ii) what geometry of idealized obstacles is the most appropriate for modeling the architecture of the network in semidilute solutions. To answer these questions we have undertaken an experimental study of sieving in semidilute solutions of polyethylene glycol (PEG) in the wide molecular weight range of 200000–800000. Native proteins of molecular weight 14–530 kDa were used as size standards in the size range conventionally applied to gel electrophoresis.

2. Materials and Methods

2.1. Proteins. Proteins used are listed in Table 1.

* Author to whom correspondence should be addressed: Bldg. 10, Rm. 6C215, NIH, Bethesda, MD, 20892-1855. Tel, 301-496-4878; FAX, 301-402-0263.

[⊗] Abstract published in *Advance ACS Abstracts*, November 15, 1996.

TABLE 1: Proteins

| name | M_r | Stokes radius ^a (nm) | source ^b | cat. no. |
|-----------------------------------|-------|---------------------------------|---------------------|-----------------|
| α -lactalbumin | 14.4 | 1.4 | Sigma | L-4385 |
| carbonic anhydrase | 29.0 | 1.85 | Sigma | C-5024 |
| ovakbumin | 43.5 | 2.2 | Sigma | A-7641 |
| bovine serum albumin | 66.0 | 2.4 | Sigma | A-8654 |
| human serum albumin | 67.0 | 2.45 | Calbiochem | 126658 |
| glucose-6-phosphate dehydrogenase | 190.0 | 3.0 | Worthington | 3981 ZFL 58P490 |
| <i>R</i> -phycoerythrin | 290.0 | 4.0 | Polysciences | 18188 |
| ferritin | 450.0 | 4.84 | Serva | 21318 |
| urease | 545.0 | 4.8 | Sigma | U-7752 |

^a Stokes radii, R , were calculated from sedimentation constants $S_{20,w}$ (Section C of ref 24), using eq 3.8 of ref 25. ^b Sigma: St. Louis, MO 63178. Calbiochem: San Diego, CA 92112. Polysciences: Warrington, PA 18976. Serva: Heidelberg, FRG D-6900. Worthington: Freehold, NJ 07728.

TABLE 2: Polyethylene Glycol

| $M_r \times 10^6$ | c^* (%) | concentration range (%) | source ^a | cat. no. |
|-------------------|-----------|-------------------------|---------------------|----------|
| 0.2 | 1.2 | 0.75 | Serva | 33126 |
| 0.4 | 0.7 | 0.75 | Serva | 33128 |
| 0.6 | 0.5 | 1.0–3.0 | Serva | 33129 |
| 1.0 | 0.35 | 0.7–1.8 | Serva | 33131 |
| 4.0 | 0.12 | 0.3–0.9 | Serva | 33134 |
| 5.0 | 0.10 | 0.3–0.9 | Serva | 33135 |
| 8.0 | 0.07 | 0.15–0.5 | Aldrich | 37,283-8 |

^a Aldrich: Milwaukee, WI 53233.

2.2. Polymers. Polyethylene glycol (PEG) specified in Table 2 was used.

The entanglement threshold, c^* , was derived by the relation $c^* = 1.5/[\eta]^{15}$ using the nominal M_r of PEG and the Mark–Houwink–Sakurada equation

$$[\eta] = KM_r^a$$

where K and a were 0.0119 (mL/g) and 0.76, respectively.¹⁶

2.3. Capillary Zone Electrophoresis (CZE). CZE was carried out on the proteins (Table 1) in PEG (Table 2) containing buffer (0.025 M CHES, 0.05 M Tris, pH 9.0), using the HPCE-2100 apparatus (Beckman Instruments, Fullerton, CA) equipped with fluorescence and ultraviolet detectors. Capillaries of 27 cm length and 100 μ m diameter were used. Ultraviolet detection at 214 nm was used except for phycoerythrin, a native fluorescent protein. Other conditions were those previously described.¹⁷

2.4. Data Processing. The program SigmaPlot (Jandel Scientific) was used for curve fitting on the Macintosh computer.

3. Results

3.1. Near-Independence of Protein Retardation of the M_r of PEG. Figure 1 shows a representative example (phycoerythrin, $R = 4.0$ nm) for the relation between the local retardation coefficient [$K_R' = \log(\mu/\mu_0)/c$]¹⁸ and PEG molecular weight at a PEG concentration of 0.75%. The transition between the dilute and semidilute regimes at 0.75% PEG is shown by the arrow. It is seen that K_R' in the semidilute PEG solution is near-independent of the M_r of PEG as indicated by the fact that in the representative case shown, K_R' is proportional to the 0.05th power of M_r . The figure also shows that this near-independence of the retardation of the M_r of PEG does not hold in the dilute polymer solution.

3.2. Linear Relationship Between the Retardation of Proteins with Radii Larger than 2 nm and the 0.75th Power

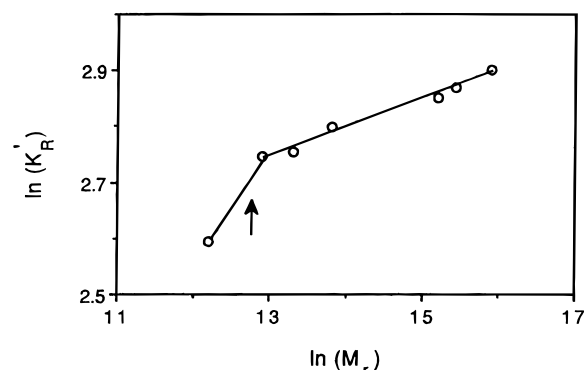


Figure 1. Near-independence of the local retardation coefficient, K_R' , of the molecular weight, M_r , of PEG in semidilute solution. In the representative case shown, that of a PEG concentration of 0.75%, the position of the arrow divides semidilute solutions (on the right) from dilute solutions (on the left). $K_R' = [\log(\mu/\mu_0)/c]$, where c = PEG concentration.²¹ Mobility, μ , and free mobility, μ_0 , of phycoerythrin ($R = 4.0$ nm) were measured by CZE (CHES–Tris buffer, pH 9, 25 °C, 370 V/cm) in the presence and absence of PEG, respectively.

of PEG Concentration. The logarithm of the relative mobilities, μ/μ_0 , of proteins varies with polymer weight fraction by a function described by a straight line for particles with radius, R , of less than 2 nm (Figure 2A) and a slightly concave curve for representative larger particles in the range of R between 2 and 5 nm (Figure 2B,C). The latter relation is linearized when the relative mobilities are plotted against the 0.75th power of the polymer weight fraction (Figure 2E,F).

Figure 2 shows the relation between retardation and PEG concentration for three proteins of 1.4, 3.0, and 4.8 nm radius as representative examples of nine proteins in the same size range studied. PEG in the abscissa refers to the entire spectrum of polymer size in the range of 600000–8000000 (Table 2) and to the sum of the data on protein retardation gathered from these variously sized polymers.

3.3. Linear Relation between K_R'' and Protein Radius. The slopes of the linear plots of $\log(\text{relative mobility})$ vs polymer weight fraction to the 0.75th power (Figure 2D,E,F), designated as K_R'' , increase linearly with R in the protein size range of $2 < R < 5$ (Figure 3).

3.4. Independence of K_R'' of Field Strength. Protein retardation, expressed as K_R'' , is independent of the field strength, E (V/cm). Although only demonstrated for a representative case of $R = 4.0$ nm and PEG M_r s of 1 and 8×10^6 , the relation is taken to hold for the entire protein and PEG size range under investigation.

4. Discussion

4.1. Relation between Particle Retardation and Polymer Molecular Weight. Let us start with the consideration of the assumption that the mean diameter of a spherical space in the polymer network, d , in eq 1 is directly proportional to the mesh size, ξ .¹⁰ In good solvents, ξ is dependent on polymer concentration c ($\xi \propto c^{-0.75}$) but independent of the molecular weight of polymer, M_r .¹¹ Thus

$$\log(\mu/\mu_0) = -(ARc^{0.75})^m \quad (4)$$

where A is a numerical constant. Therefore, the retardation at a fixed polymer concentration expressed as a local retardation coefficient, K_R' ,¹⁸ must be molecular weight independent.

The experimental observation is in reasonable agreement with that expectation: Figure 1 shows that the dependence of local retardation on PEG molecular weight is slight, namely $K_R' \propto M_r^{0.05}$ and may therefore be neglected.

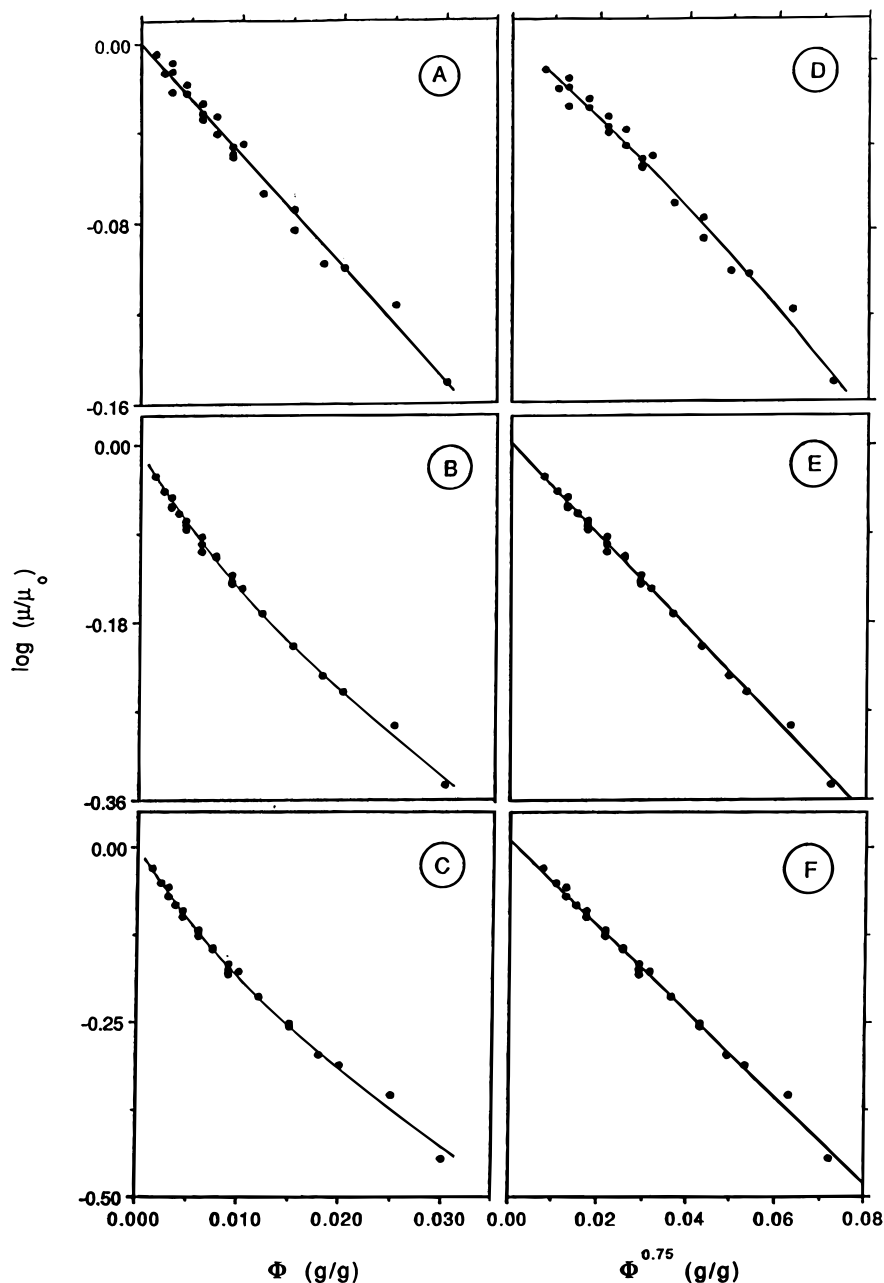


Figure 2. Polymer concentration dependence of retardation in semidilute PEG solutions. The retardation, expressed as μ/μ_0 , of three representative particles with radii 1.4 nm (panels A, D), 3.0 nm (panels B, E), and 4.8 nm (panels C, F) is shown as a function of polymer weight fraction, Φ . Conditions of CZE as in Figure 1. The curves in each panel are composed of experimental points obtained from measurements in PEG solutions of different M_r and concentration (Table 2). The dimensionless measure of concentration, the polymer weight fraction Φ , has been used for convenience.

The sources of the weak increase are not clear. Perhaps, the solvent used (25 mM CHES, 50 mM Tris, pH 9.0) does not provide a “good solvent” for PEG at the experimental temperature (25 °C). Another possible reason for the slight dependence of K_R' on the M_r of PEG is that the fixed polymer concentration of 0.75% approaches the entanglement threshold, c^* , as the PEG molecular weight is decreased (Figure 1 and Table 1). Such approximation toward c^* should give rise to a decreasing lifetime of entanglements leading to the observed slight reduction of the retardation.

4.2. Relation between Particle Retardation and Polymer Concentration. In accordance with the molecular weight independence of retardation, K_R' values of a particle at various polymer concentrations would be expected to fit onto a single curve comprising K_R' data for all of the various polymer M_r s used. Figure 2 (A–C) demonstrates that the experimental findings are in good agreement with that expectation. It

should be noted that the concentrations of PEG in all of the data of Figure 2 have been at least two times higher than c^* (Table 1).

The plot of $\log(\mu/\mu_0)$ vs Φ was found to be nonlinear for particles larger than 2 nm in radius (see the representative plots in Figure 2B,C) and rather linear for particles of smaller radii (see the representative plot in Figure 2A). The nonlinear dependence of $\log(\mu/\mu_0)$ on polymer concentration can be linearized by plotting $\log(\mu/\mu_0)$ vs $\Phi^{0.75}$ (Figures 2E,F). Hence it appears that exponent m in eq 4 has to be equal to 1 for “large” particles of $R > 2$ nm and increases if $R < 2$ nm.

In the range of the linear relation between $\log(\mu/\mu_0)$ and $\Phi^{0.75}$, the retardation can be expressed by the slope of the plot of that relation (a retardation coefficient). In analogy to the terminology of gel electrophoresis,^{6,7} that retardation coefficient in semidilute solutions, K_R'' , may be defined as $-\log(\mu/\mu_0)/\Phi^{0.75}$. K_R'' depends on particle radius and solvent-polymer interactions

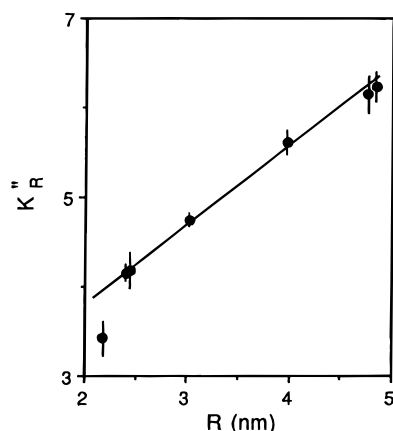


Figure 3. Linear relation between the retardation coefficient, K_R'' , and particle radius, R , in electrophoresis using semidilute solutions of PEG. K_R'' is defined as $d[\log(u/\mu_0)]/d(\Phi^{0.75})$ as illustrated by the slopes of the lines in panels E and F of Figure 2. K_R'' was measured under the conditions described for Figure 2.

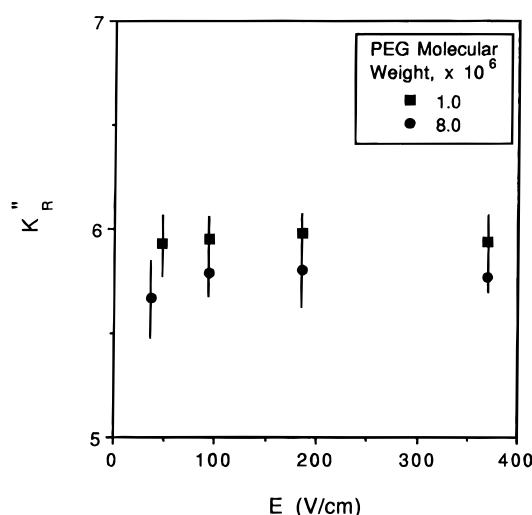


Figure 4. Independence of K_R'' of field strength. Conditions of CZE of phycoerythrin are as described for Figure 1, except that the electric field strength was varied as shown. Two representative cases (PEG of $M_r = 4\,000\,000$ and $8\,000\,000$) are depicted. PEG concentrations varied as shown in Table 2.

but is independent of concentration and molecular weight of the polymer.

4.3. Dependence of Retardation on Particle Radius. When m in eq 1 equals 1 for particles of $R > 2$ nm, this results in a linear dependence of K_R'' on R . The plot in Figure 3 depicts such a relation. When $R < 2$ nm, the relation between polymer concentration dependent retardation and particle size in the semidilute solutions is thought to approach that in a gel (Figure 2A and eq 3); however, the data are too few to allow for a firm conclusion in that regard.

4.4. Dependence of the Retardation on Electric Field Strength. The particle penetration into a gel by occupation of available spaces between obstacles implies the field strength independence of retardation.^{6,7,14} Therefore, under the assumption of the equivalence of “pore size” in gels and “mesh size” in semidilute polymer solutions,¹⁰ the penetration into a network constituted by entangled polymers can be expected to be independent of field strength, E , as well. Figure 4 demonstrates that the experimental findings agree with that expectation.

4.5. Geometry of Obstacles in a Polymer Network. To date, the molecular sieving of rigid particles in electrophoresis has been considered as the partitioning of particles between spaces (“pores”) formed by surfaces of the obstacles constituting

the network.^{4,6,7} It has been described in terms of exclusion due to a surface-overlap phenomenon (19) and requires therefore the postulate of particular idealized geometric shapes of the obstacle. Historically, the mathematical model of Ogston⁵ has been the one applied to gel electrophoresis.⁶ The idealized shapes of the obstacle considered by that model have been the “point” (0-D gel with obstacle length approaching 0!), the “fiber” (1-D gel consisting of straight, rigid obstacles of infinite length!) and the “plane” (2-D gel) (ref 6; see also Figures 14 and 16 of ref 20). Although the random fiber model would appear physically realistic both for gels and semidilute solutions, rigorously none of those purely geometric models can be thought to describe a real gel or a polymer solution composed of interacting flexible polymer chains. In gels, the experimental findings of the relation between retardation and particle radius agree with the predictions of the model for a 1-D obstacle network (a linear relation between mobility and gel concentration and between the square root of the retardation coefficient and the particle radius). By contrast, the experimental findings for electrophoresis in semidilute polymer solutions of a proportionality between retardation coefficient and particle radius are consistent with the model of a “2-D obstacle network” of randomly distributed planes (Figure 3 and Appendix to ref 21). The consistency of gels and polymer solutions with different idealized models raises the question whether they may be a corresponding difference in real systems and, if so, what that difference may be. That difference is likely to be due to the cross-linking of gels which restricts the degrees of freedom for the motions of polymer chains. In polyacrylamide gel it results in a progressive structural heterogeneity with increasing concentration of cross-links.²² Recently it has also been shown by neutron and light scattering²³ that the cross-linked poly(vinyl alcohol) hydrogel is characterized by static concentration fluctuations not observed in the corresponding uncross-linked semidilute polymer solution. Thus, the random plane model may reflect the physical reality of a reduced heterogeneity, compared to a cross-linked gel, in the distribution of polymer chains in a semidilute solution.

Conclusion

With respect to the electrophoretic migration of particles of 2 to, at least, 5 nm radius (protein molecular weight of 40–500 kDa), a semidilute polymer solution may be viewed as a porous network with the properties of an idealized system of obstacles composed of random planes. The average spacing between planes is considered to equal the screening length, and the size-dependent retardation (molecular sieving) can be described by

$$\log(u/\mu_0) = -(ARc^{0.75}) \quad (5)$$

where A is a constant dependent on solvent and type of monomer and c is the polymer concentration.

References and Notes

- (1) Tietz, D.; Gottlieb, M. H.; Fawcett, J. S.; Chrambach, A. *Electrophoresis* **1986**, *7*, 217.
- (2) Grossman, P. D. *Capillary Electrophoresis: Theory and Practice*; Academic Press: San Diego, CA, 1992; pp 215–236.
- (3) Noolandi, J. *Adv. Electrophor.* **1992**, *5*, 1.
- (4) Arvanitidou, E.; Hoagland, D.; Smisek, D. *Biopolymers* **1991**, *31*, 435.
- (5) Ogston, A. G. *Trans. Faraday Soc.* **1958**, *54*, 1754.
- (6) Rodbard, D.; Chrambach, A. *Proc. Natl. Acad. Sci. U.S.A.* **1970**, *65*, 970.
- (7) Rodbard, D.; Chrambach, A. *Anal. Biochem.* **1971**, *40*, 95.
- (8) Slater, G. W.; Guo, H. L. *Electrophoresis* **1996**, *17*, 977.
- (9) Wheeler, D. L.; Chrambach, A. *Biopolymers* **1995**, *35*, 179.

- (10) Grossman, P. D.; Soane, D. S. *Biopolymers* **1991**, *31*, 1221.
- (11) De Gennes, P. G. *Macromolecules* **1976**, *9*, 587.
- (12) Viovy, J.-L.; Heller, C. *Capillary Electrophoresis in Analytical Biotechnology*; CRC Press: Boca Raton, FL, 1995.
- (13) Viovy, J.-L.; Duke, T. *Electrophoresis* **1993**, *14*, 322.
- (14) Morris, C. J. O. R. *Protides of the Biological Fluids*; Elsevier: New York, 1967; p 543.
- (15) Bohdanecky, M.; Kovar, J. *Viscosity of Polymer Solutions*; Elsevier: Amsterdam, 1982; p 220.
- (16) Molyneux, P. *Water-Soluble Synthetic Polymers: Properties and Behavior*; CRC Press: Boca Raton, FL, 1982; p 26.
- (17) Radko, S. P.; Garner, M. M.; Caiafa, G.; Chrambach, A. *Anal. Biochem.* **1994**, *223*, 82.
- (18) Tietz, D.; Chrambach, A. *Electrophoresis* **1986**, *7*, 241.
- (19) Giddings, C.; Kucera, E.; Russell, C. P.; Myers, M. N. *J. Phys. Chem.* **1968**, *72*, 4397.
- (20) Chrambach, A. *Mol. Cell. Biochem.* **1980**, *29*, 23.
- (21) Tietz, D.; Chrambach, A. *Electrophoresis* **1992**, *13*, 286.
- (22) Mallam, S.; Horkay, F.; Hecht, A.-M.; Geissler, E. *Macromolecules* **1989**, *22*, 3356.
- (23) Horkay, F.; Hecht, A. N.; Geissler, E. *Macromolecules* **1994**, *27*, 1795.
- (24) Sober, H. A. *Handbook of Biochemistry*; CRC Press: Cleveland, OH, 1973.
- (25) Price, C. A. *Centrifugation in Density Gradients*; Academic Press: New York, 1982; p 37.

JP9612339